MedChemComm

Accepted Manuscript

ROYAL SOCIETY OF CHEMISTRY

www.rsc.org/medchemcomm

Bisimidazoline arylamides binding to the DNA minor groove. *N*1-hydroxylation enhances binding affinity and selectivity to AATT sites†

Carlos H. Ríos Martínez[a,b], Laura Lagartera[a], Cristina Trujillo[c], and Christophe Dardonville[a]*

[a] *Instituto de Química Médica, IQM–CSIC, Juan de la Cierva 3, 28006 Madrid, Spain.*

[b] *INDICASAT-AIP, Edificio 219, Clayton, City of Knowledge, Ciudad de Panamá, República de Panamá.*

[c] *School of Chemistry, Trinity Biomedical Sciences Institute, Trinity College Dublin, 152-160 Pearse St., Dublin 2, Ireland.*

Bisimidazoline arylamides and related compounds are high affinity DNA minor groove binders with a preference for AT over GC-rich DNA. However, further selectivity between different classes of AT-sites (e.g., CGAATTCG, CATATATAT) is not always observed with these series. In this work, we wanted to understand the effect of imidazoline ring *N*-substitution on binding to DNA AT-sites. The structure-affinity relationships of a series of structurally related bisimidazoline compounds were studied by UV titrations and surface plasmon resonance (SPR) experiments using fish sperm DNA and different hairpin oligonucleotides. We found that in this series the presence of *N*1-OH groups enhances the binding affinity to dsDNA CGAATTCG oligonucleotide resulting in higher selectivity for dsDNA containing AATT over $(AT)_4$ sequences. The docking models showed that the *N*-hydroxy derivatives bind in a more planar conformation with the CGAATTCG DNA sequence, display more favorable van der Waals interactions, and show additional H-bonds with the bases and the sugar–phosphate backbone.

Introduction

The research efforts in the past decades have led to a growing understanding of the DNA structure and drug-DNA interactions. Specific binding to DNA is thought to be achieved either by the formation of hydrogen bonds between the ligand and the base pairs of DNA or to the recognition of a specific sequence-dependent shape of the DNA double helix.[1] In AT-rich DNA, ligand-induced narrowing of the minor groove and changes in bending of the DNA helix upon complex formation contributes to the binding of minor groove agents.[2-4] Narrow minor grooves, often associated with the presence of A-tracts, strongly enhance the electrostatic potential of the DNA.[5] These sequence-specific properties of DNA are used by many DNA–binding proteins[1] and minor-groove-targeting compounds as recognition mechanism. Hence, most of the minor-groove ligands share some structural characteristics (i.e., positive charge(s), linked rather than fused aromatic or heteroaromatic rings, crescent shape –"isohelicity"– matching the curve of the groove) that allow the ideal match between the ligand and the groove through van der Waals and hydrogen bonding (HB) interactions.[6]

Minor groove binders are especially interesting DNA-interacting compounds for antimicrobial drug design because they are sequence selective (in contrast to intercalators which are sequence neutral), principally binding to A/T-rich DNA duplexes. This selectivity is particularly relevant in the case of parasitic pathogens such as trypanosomes which mitochondrial genome contains a high proportion of A/T-rich DNA sequences.[7] Due to their unique structural features,[8] the A/T-rich minicircles of mitonchondrial kinetoplast DNA (kDNA) appear to be the target for drug interaction.[3, 4, 7]

In previous studies, we have discovered diphenyldicationic compounds **1**–**5** (Chart 1) that showed excellent in vivo activity against African trypanosomes (*T. b. rhodesiense*) in mouse models of sleeping sickness.[9-12] The binding interaction of **5** with the minor groove of the all-AT DNA sequence $d(AAAATTTT)_2$ and with the self-complimentary nucleotide $d(CTTAATTCGAATTAAG)_2$ was demonstrated by X-ray crystallography.[13, 14] Nagle et al. showed that the arylamide derivatives **1** and **2** bound strongly and selectively to AT oligonucleotides with a slight preference (2- to 3-fold) for the dsDNA CGAATTCG vs CATATATAT sequences.[15] The same group observed that *N*-substitution of the guanidinium groups by hydroxyl radicals abolished almost completely the binding affinity of these ligands.[16] Similarly, reduction in DNA binding affinity was observed with diamidine and bisguanidines analogues which cationic moieties were derivatized with *N*-alkyl groups.[10, 17-19]

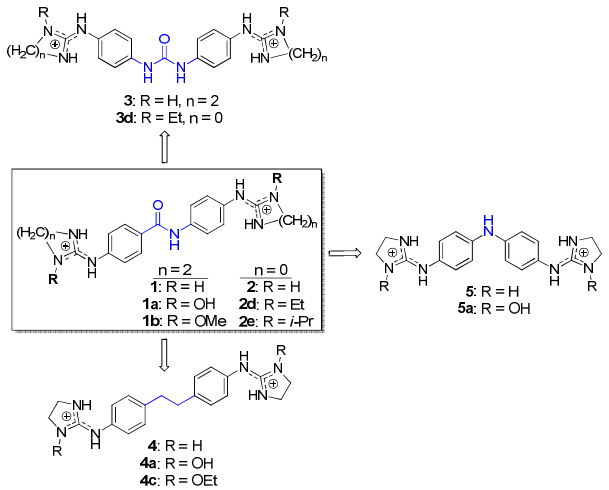

Chart 1. Structure of the bisimidazoline arylamides (**1**, **1a**, and **1b**) and analogues (**2**–**5**) used in this study.

The goal of the present study was to understand the effect of imidazoline ring *N*-substitution on arylamide binding to the minor groove of AT-rich DNA. As the here presented results together with the many other studies of minor groove binders point to the involvement of shape-recognition by DNA, it was important to determine the selectivity of binding to different DNA sequences (i.e., DNA shapes). Hence, the binding of a series of ten closely related guanidine and imidazoline compounds (Chart 1) to unspecific fish-sperm DNA, and dsDNA containing CGAATTCG, CATATATAT, and CGCGCGCG was studied by UV spectrophotometry, and surface plasmon resonance (SPR)–biosensor experiments. Molecular docking studies using representative crystal structures of both dsDNA oligonucleotides CGAATTCG (pdb: 1ENN) and CATATATAT (pdb: 3TED) were carried out to rationalize these findings.

Results and discussion

Spectrophotometric Titrations. Compounds **1a** and **1b** have a strong absorption band at 280 nm, compounds **4a** and **4c** have a strong absorption band < 250 nm and a weak absorption in the 300–360 nm region, and **5a** has a strong absorption band at 296 nm. These absorption spectra were strongly perturbed when the bisimidazolines formed a complex with unspecific fish-sperm (FS) DNA (Figure 1). Compounds **1a** and **1b** had isoabsorptive behaviours, as well as **4a** and **4c**. For all of the compounds, a clear isosbestic point was observed during the titration, indicating a single dominant mode of binding to FS DNA. A weak hypochromicity (9–34%) at the compounds peak wavelength was observed upon binding which is consistant with minor groove binding.

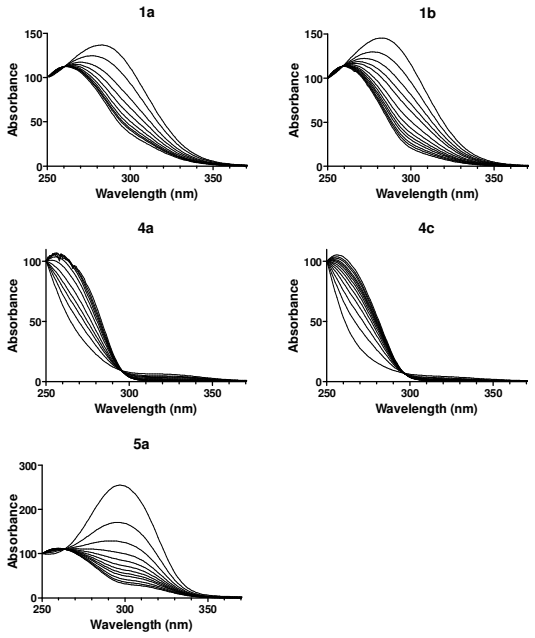

Fig. 1 UV titration of **1a, 1b, 4a, 4c,** and **5a** (30 μM) with FS DNA in 10 mM phosphate buffer (pH 7) at 25 ºC. FS-DNA concentrations ranged from 0 to 7.89×10^{-5} M (**1a**), 0 to 1.8×10^{-4} M (**1b**), 0 to 2.89×10^{-4} M (**4a**), 0 to 1.37×10^{-4} M (**4c**), and 0 to 1.16×10^{-4} M (**5a**) from top to bottom.

Binding of **1a** to the specific dsDNA CGAATTCG [AATT] hairpin oligonucleotide produced strong alterations of the UV spectra (i.e. similar to that observed with FS DNA) whereas binding to dsDNA CATATATAT [$(AT)_4$] and CGCGCGCG [$(CG)_4$] sequences induced much weaker changes (Figure S1). These results suggested that **1a** bind more specifically to the dsDNA containing AATT. The absorption spectra were strongly perturbed when **5a** formed a complex with dsDNA containing AATT (Figure S1). An isosbestic point at 325 nm indicated a single mode of interaction with the AATT hairpin. A new band attributed to the compound-DNA complex appeared at approximately 335 nm. Upon interaction with the $(AT)_4$ hairpin, an isosbestic point at 335 nm was observed and a weak band attributed to the compound-DNA complex appeared at 340 nm. In contrast, no isosbestic point or new band was observed in the titration with the $(CG)_4$ sequence. This is consistant with the absence of strong interaction of **5a** with CG-rich DNA.

SPR–Biosensor Experiments. The DNA binding affinity and stoichiometry of the compounds was determined using SPR–biosensor experiments with three DNA hairpin duplexes [i.e., AATT, $(AT)_4$, $(CG)_4$] immobilized on a biosensor chip surface.[20, 21] The SPR response (RU) at equilibrium in the SPR sensorgrams (i.e., in the plateau region) was converted to r (moles of bound compound per mole of DNA hairpin duplex; r = RU / RU_{max}) and was plotted against the free compound concentration, C_f, flowing on the chip surface (i.e., immobilized DNA hairpin) (Figure 2). The binding constants were determined by fitting the values to single site or two-site binding models according to Equation 1 (see experimental part). When two binding sites exist for a given DNA sequence, only the primary binding constant is given.

Structure–Affinity Relationships. SPR experiments showed that none of the compounds bind significantly to the dsDNA containing $(CG)_4$ sequences as expected for this class of minor groove binders. The bisimidazoline arylamide derivatives (**1**, **1a**, and **1b**) were the strongest DNA binders. However, different binding behaviors and affinities were observed depending on the spacer linking both phenyl groups and the *N*1-substituent on the imidazoline rings (Table 1). The main SAR results are presented below.

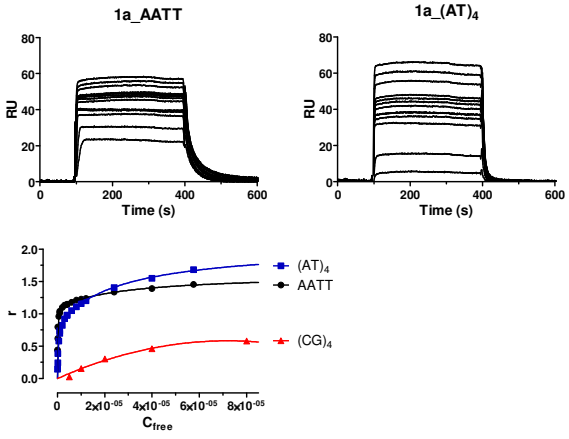

Fig. 2 SPR binding affinity. (1) Sensorgrams for binding of **1a** to CGAATTCG [AATT] and CATATATAT [$(AT)_4$] hairpin duplexes using increasing concentrations of ligand in the range 0.05–57.6 μM (from bottom to top). (2) SPR binding plots of **1a** for AATT, $(AT)_4$ and CGCGCGCG [$(CG)_4$] hairpins.

*Effect of linker modification: ethylene, urea and amino analogues***.** Bisimidazolines (**1**, **1a**, and **1b**) and bisguanidine (**2**, **2d**, and **2e**) arylamide derivatives showed the highest binding affinities for AT oligonucleotides with a slight preference for dsDNA containing AATT over $(AT)_4$ sequences (1.5 to 2-fold). Binding of all of the compounds but **3d** to AT sequences was adjusted to a two-site binding model. Primary binding

constants were about 100 times higher than secondary binding constants. Compounds with a urea linker (**3**, **3d**) displayed only weak affinity for DNA (K_D > 8.3 ×10^{-6} M) with no sequence selectivity between AT-oligonucleotides and moderate selectivity over CG for **3** (~ 10- to 50-fold). These results together with the ratio of moles of bound compound per mole of DNA hairpin duplex (r ≥ 2 for most sequences) are consistent with an intercalation mode of binding and/or external electrostatic interactions for the urea derived compounds **3** and **3d**.

Binding affinities of the ethylene linked compounds (**4**, **4a**, and **4c**) were 10- to 15-fold weaker than that of the arylamide analogues (**1a-b** – **2d-e**) but 2- to 4-times stronger than the urea analogues (**3**, **3d**). Primary binding of **4** and **4a** to AT sequences was 5 to 10-fold and 30 to 50-fold stronger than the secondary binding, respectively. The amino-linked compounds **5** and **5a** bound to dsDNA containing AATT more weakly than the arylamide analogues **1** and **1a** (15- and 7-fold, respectively).

All together, these results clearly demonstrate the strong influence of the linker on DNA binding mode and affinity, and that the arylamide scaffold ("amide linker") is a privileged scaffold for AT-sites DNA binding independently of the cationic moieties present in the molecule.[15]

Effect of "imidazoline ↔ guanidine" group modification. Guanidines bound somewhat less strongly than imidazoline analogues. Substitution of the guanidine with alkyl groups (**2d**, **2e**) decreased the binding affinity for AT sequences (6 to 9-fold).[10] These results agree with previous studies showing that bisimidazolines of this class bind more strongly and selectively to AT-rich DNA than their guanidine counterparts, probably due to more favorable van der Waals interactions of the imidazoline rings with the minor groove.[11, 12, 14] Crystallographic studies of **5** bound to dsAT-DNA have shown that these favorable interactions also promote bifurcated hydrogen bonds between the imidazoline endocyclic nitrogens and thymine and adenine atoms in opposite DNA strands that facilitate recognition of both strands of the DNA within the minor groove.[13, 14]

Effect of N1-substituents on AT-site selectivity. The most remarkable effect of the imidazoline *N*1 substituents was observed with hydroxyl groups. A two-fold increase in affinity towards dsDNA containing AATT was observed for **1b** in comparison with the unsubstituted parent compound **1** (K_{AATT} = 0.077 × 10^{-6} M and 0.166 × 10^{-6} M, respectively). In contrast, no change in binding affinity to the dsDNA CATATATAT sequence was observed. Thus, *N*1-hydroxylation resulted in a 3.5-fold selectivity enhancement for dsDNA containing AATT sequences over $(AT)_4$.

Table 1. DNA binding constants determined by SPR for dsDNA containing AATT, $(AT)_4$, and $(CG)_4$ sequences[‡]

Structure	Cmpd	R	dsDNA CGAATTCG K_D (×10^{-6}M)[a]	dsDNA CATATATAT K_D (×10^{-6}M)[a]	dsDNA CGCGCGCG K_D (×10^{-6} M)
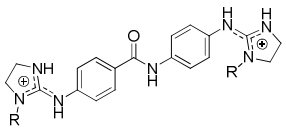	**1**	H	0.166[b]	0.307[b]	>10[c,d]
	1a	OH	0.077	0.273	18.5
	1b	OMe	0.256	0.351	>10[c]
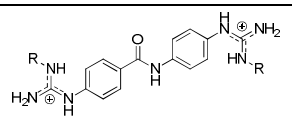	**2**	H	0.141[e]	0.556[e]	>10[c]
	2d	Et	1.23[f]	1.92[f]	>10[d]
	2e	^{i}Pr	1.02[f]	2.5[f]	>10[d]
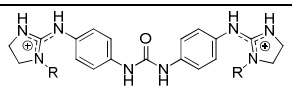	**3**	H	11.6	8.06	400–158.7
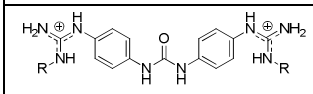	**3d**	Et	>29	>29	[c]
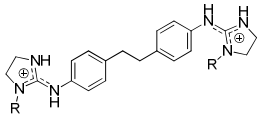	**4**	H	2.78	4.35	19.6
	4a	OH	0.870	4.0	76.9
	4c	OEt	>29	>29[d]	>29
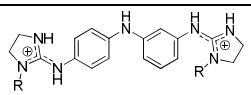	**5**	H	2.70	2.17[g]	[c]
	5a	OH	0.568	1.79	66.7

[‡] dsDNA hairpins used in the study (the loop is underlined): 5'-biotin-CGAATTCGTCTCCGAATTCG-3' [AATT], 5'-biotin-CATATATATCCCCATATATATG-3' [$(AT)_4$], and 5'-biotin-CGCGCGCGTTTTCGCGCGCG-3' [$(CG)_4$]

[a] Primary binding constant for fitting to a two-site binding model. [b] Nagle et al[15] reported similar binding constants for AATT and $(AT)_4$ oligonucleotides (0.107×10^{-6} M and 0.210×10^{-6} M, respectively). [c] There is not enough signal to noise ratio to get a binding constant for this hairpin oligonucleotide. [d] Nonspecific binding. [e] Taken from reference [15]. [f] Taken from reference [10]. [g] Taken from reference [14].

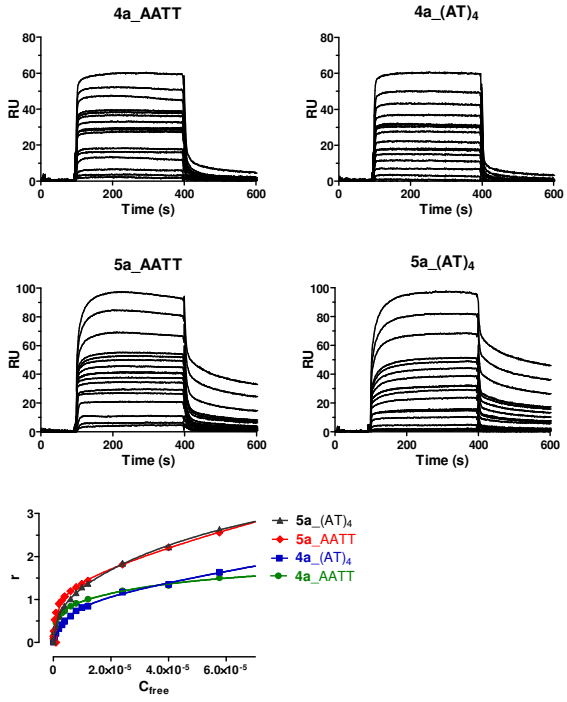

Fig. 3 (1) Sensorgrams for binding of **4a** and **5a** to CGAATTCG [AATT] and CATATATAT [$(AT)_4$] hairpin duplexes using increasing concentrations of ligand in the range 0.05–57.6 µM (from bottom to top). For **5a**, the shape of the sensorgram clearly shows a different profile with a slow binding and dissociation process. (2) SPR binding plots of **4a** and **5a** for AATT and $(AT)_4$ hairpins.

The same results were observed for the ethylene linked *N*-hydroxy derivative **4a** (K_{AATT} = 0.87 × 10^{-6} M vs 2.78 × 10^{-6} M for the unsubstituted parent compound **4**) and the amino linked compound **5a** (K_{AATT} = 0.568 × 10^{-6} M vs 2.70 × 10^{-6} M for the parent compound **5**) showing that this effect may possibly be generalised to other bisimidazolines. On the contrary, introduction of alkoxy groups (OMe, OEt) was detrimental to binding to AT DNA indicating that the OH group of *N*-hydroxyimidazolines is probably involved in additional stabilizing H-bonds interactions with the DNA minor groove.

Noteworthy is the binding behaviour of the *N*-hydroxy derivative **5a**. The kinetics of binding to AT sequences is rather different from the rest of the compounds with a slow dissociation process (Figure 3). Since the stoichiometry (r value) is > 2, the results suggest a different, more complex, binding mode to AT sequences. We recently made similar observations with a 39 bp dsDNA containing GAATAATCGCGATTATTC which formed a slow-binding (k_{on} = 38 $M^{-1}s^{-1}$) long-lasting (k_{off} = 0.00265 s^{-1}) complex with **5a** (Dr. L. Campos, personal communication). This result is important as longer drug–target residence time is considered a key driving-force of the pharmacodynamic activity and efficacy of many drugs *in vivo*.[22-25]

Molecular Docking Studies. In order to understand the reasons behind the increased affinity of the *N*-hydroxy derivatives, docking experiments were run using the crystal structures of d(GCGAATTCG) [1ENN][26] and d(CCATATATATGC) [3TED][27] as template for the dsDNA containing AATT and $(AT)_4$ sequences, respectively. The docking experiments were able to rank correctly (i.e. in agreement with the experimental values) the ligands into two groups of high (**1a**>**5a**>**1**≈**5**≈**4a**>**4**) and low (**3**>**4c**>**3d**) predicted binding affinity, respectively (Table S1). However, the differences in binding affinities were too small (i.e. within the limits of the standard error of the calculation) and did not allow us to extract useful conclusions in relation with the increased affinity of the *N*-hydroxy derivatives for the dsDNA containing AATT. Hence, the detailed study of the interactions of lead **1** and its *N*-hydroxy analogues **1a** with both AATT and $(AT)_4$ sequences was carried out.

In contrast to the dsDNA containing CATATATAT where the ligands bind in a more twisted conformation, the phenyl rings of **1** and **1a** adopt a more coplanar conformation when bound to the dsDNA CGAATTCG (Figures S3–S6). These results agree well with the induced-fit observed with this kind of ligand when bound to a narrow minor groove.[14] An analysis of the non-covalent interactions[28] in the ligand-DNA complexes showed that **1** and **1a** form more (and larger) weak attractive interactions with the dsDNA containing CGAATTCG compared to CATATATAT (Figure S7) which is consistent with the values of binding affinities measured experimentally.

Finally, the analysis of the HB interactions in the complexes of **1** and **1a** with CGAATTCG and CATATATAT oligonucleotides showed distinctive patterns depending on the presence of the *N*-OH group or not (Figures 4 and S8). For instance, **1** forms two HBs (2.19 and 2.50 Å) with the phosphate groups of the sugar–phosphate backbone and 1 HB (2.35 Å) with the O4' atom of the A5 deoxiribose of the dsDNA GCGAATTCG (Figure S8_A).

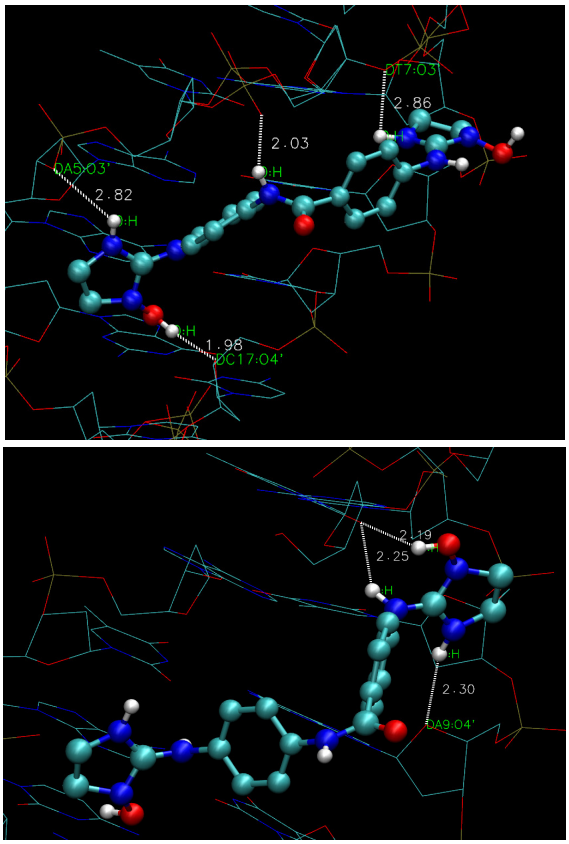

Fig. 4 Plot of hydrogen bonds (HB) interactions for **1a** docked with d(GCGAATTCG) (top) and d(CCATATATATGC) (bottom) oligonucleotides.

In contrast, **1a** forms a strong HB between the OH group and the O4' atom of the C17 deoxiribose (Figure 4, 1.98 Å) and three HBs (2.03, 2.82, and 2.86 Å) with phosphate groups of the sugar–phosphate backbone (i.e. with the amide NH and the imidazoline NH from both sides of the molecule, respectively). With the d(CCATATATATGC) oligonucleotide, **1a** forms 1 HB (2.30 Å) with the O4' atom of the A9 deoxiribose and a bifurcated HB between thymine T6 and the imidazoline N(2)H (2.25 Å) and N(1)OH (2.19 Å) (Figure 4) which is absent in the complex with compound **1** (Figure S8_C).

As a whole, the docking studies indicate that the better fit of the *N*-hydroxy derivatives in the narrow minor groove of dsDNA containing AATT may be due to favorable van der Waals interactions with the walls of the groove, a more planar conformation of the bound ligand, and additional stabilizing H-bonds between the *N*-OH groups and sugar residues and/or the base edges.

Conclusions

We have shown that *N*-substituted diphenyl-based bisimidazoline compounds bind strongly to dsDNA, preferentially to A/T containing oligonucleotides. The presence of one hydroxyl substituent on each imidazoline endocyclic nitrogen (*N*1-OH) results in an increase in binding affinity for the dsDNA containing AATT sequence and no change in affinity for dsDNA containing $(AT)_4$. This is translated into an increase in sequence selectivity for dsDNA CGAATTCG (3.5-fold). This effect, which seems to be general for this family of imidazoline compounds (e.g, **1a**, **4a**, and **5a**) differs from that observed with *N*-hydroxy guanidine analogues that were found to bind poorly to DNA.[16] Since the dsDNA sequence CGAATTCG has a very narrow minor groove of 3.5–4.0 Å in the center of the sequence (*vs.* 5.16–6.79 Å for ATAT) and a concomitant higher electrostatic potential,[5] selective binding of the *N*-hydroxy bisimidazolines seems to derive from a tighter fit to this narrower groove.

Remarkably, in the case of **5a**, the introduction of OH substituents increases the affinity for dsDNA CGAATTCG but also results in a different stochiometry (i.e. drug/DNA, 2:1 vs 1:1 for **5**) and an increased residence time on the DNA. Because longer half-life of the drug-target complex will minimize binding to off-target proteins, this kinetic selectivity may improve the therapeutic index of **5a**.[23, 24] Hence, further studies of this compound are warranted.[29]

Experimental

Syntheses of compounds **1**,[11] **1a**,[9] **1b**,[9] **2**,[11] **2d**,[10] **2e**,[10] **3**,[11] **3d**,[9] **4**,[30] **4a**,[9] **4c**,[9] **5**,[31] and **5a**[32] have been described previously.

UV titrations. UV-vis spectra were measured on a Perkin–Elmer Lambda 35 UV–vis spectrophotometer in a 1.5 mL quartz cuvette (1 cm pathlength) in 10 mM phosphate buffer (pH 7) previously degassed by sonication. A stock solution of FS-DNA in 5 mL of phosphate buffer was prepared and shaken gently for 1 h. The concentration of FS-DNA stock solution (C = 780 µM) was worked out from the following equation: $Abs_{260} = 100 \times C \times d \times \varepsilon_{260}$ using the extinction coefficient 12800 $M(bp)^{-1}.cm^{-1}$ at 260 nm for FS-DNA.[33]

The DNA oligonucleotides 5'-CGAATTCGTCTCCGAATTCG-3' [AATT], 5'-CATATATATCCCCATATATATG-3' $[(AT)_4]$, and 5'-CGCGCGCGTTTTCGCGCGCG-3' $[(CG)_4]$ were purchased from Eurofins MWG Operon with HPLC purification. They were stored at -20 ºC as 100 µM stock solutions in phosphate buffer (pH 7) containing 1 mM EDTA + 100 mM NaCl until use. Before the titration experiments, the oligonucleotides were diluted 10× with phosphate buffer (pH 7) + 100 mM NaCl, heated at 90 ºC in a water bath for 10 minutes, and immediately chilled with ice to favour hairpin formation.

Stock solutions of the compounds **1a**, **1b**, **4a**, **4c**, and **5a** (C = 30 µM and C = 2.5 µM in phosphate buffer) were prepared from 1 mM stock solutions in DMSO by dilution with 10 mM phosphate buffer. The final amount of DMSO in the stock solution was 3%. Spectrophotometric titrations were performed by sequential addition of aliquots of FS DNA solution (C = 780 µM) to 800 µL of the compound (C = 30 µM) or hairpin oligonucleotide (C = 10 µM) to 500 µL of the compound (C = 2.5 µM) until saturation was observed. The experiments were performed at 25 ºC. The spectra were normalized and plotted with GraphPad (Prism).

SPR studies. SPR experiments were performed at 25 ºC with a Biacore X–100 apparatus (GE Healthcare, Biacore AB, Uppsala, Sweden) in MES buffer (10 mM 2-(*N*-morpholino)ethanesulfonic acid, 1 mM EDTA, 100 mM NaCl, 0.005% surfactant P20, pH 6.25). The 5'-biotin labeled DNA hairpins AATT, $(AT)_4$, and $(CG)_4$ were purchased from Sigma-Aldrich with HPLC purification, dissolved in the experiment buffer and used as such. The SPR measurements were carried out as described.[10]

The number of binding sites and the binding constants at equilibrium were obtained from fitting plots of r (r = RU / RU_{max}) against C_f. The maximum expected response (RU_{max}) per bound compound at equilibrium was calculated using a refractive index value of 1.4 as reported for similar compounds.[34] Results of binding constants were obtained by fitting SPR results to a one site ($K_2 = 0$) or two-site binding model according to equation 1:

$$r = (K_1C_f + 2K_1K_2C_f^2) / (1 + K_1C_f + K_1K_2C_f^2) \qquad (1)$$

where r is the moles of bound compound per mole of DNA hairpin duplex, K_1 and K_2 are microscopic binding constants, and C_f is the free compound concentration at equilibrium.[20, 35]

Computational Details. All compounds have been optimized using the Gaussian09[36] package at the B3LYP[37, 38] computational level with the 6–311++G(d,p)[39] basis sets. The effect of water solvation was then accounted using the SCFR-PCM approach implemented in the Gaussian09 package including dispersing, repulsing and cavitation energy terms of the solvent in the optimization.

A molecular docking study was undertaken using the AutoDock Vina 1.1.2 modelling software.[40] Compounds were docked into representative crystal structures of both dsDNA containing CGAATTCG [i.e. $d(GCGAATTCG)_2$: pdb 1ENN][26] and CATATATAT [i.e., CCATATATATGC, pdb 3TED].[27] The structures were imported into the AutoDock Vina 1.1.2 modelling software and all crystallographic water molecules and other small molecules were removed as they were located away from the ligand-binding regions. AutoDockTools 1.5.6 was used for establishing the Autogrid points as well as visualization of docked ligand–nucleic acid structures. The target site on the nucleic acid was specified to encompass the entire minor groove site. The grid center was also established by centering the grid box on the minor groove site. The Non Covalent Interactions (NCI) index, based on the reduced gradient of the electron density, has been calculated to identify attractive and repulsive interactions with the NCI program[28] and plotted with the VMD program.[41]

Acknowledgements

C.R. was recipient of a PhD fellowship for the government of Panama (SENACYT grant BIDP-2008-030). The assistance of Silvia Soto Alvarez with the SPR experiments and Eden Gebreselassie with UV experiments is gratefully acknowledged. We thank Dr N. Jagerovic, Dr P. Goya, and Dr. Alkorta for logistical collaboration.

†Electronic Supplementary Information (ESI). Spectrophotometric titration with AATT, $(AT)_4$, and $(CG)_4$ hairpin oligonucleotides (Figure S1); Docking studies: Table S1 and Figures S2–S8. See DOI:

Notes and references

1. R. Rohs, S. M. West, A. Sosinsky, P. Liu, R. S. Mann and B. Honig, *Nature*, 2009, **461**, 1248-1253.
2. M. Rettig, M. W. Germann, S. Wang and W. D. Wilson, *ChemBioChem*, 2013, **14**, 323-331.
3. D. S. Tevis, A. Kumar, C. E. Stephens, D. W. Boykin and W. D. Wilson, *Nucleic Acids. Res.*, 2009, **37**, 5550-5558.
4. R. A. Hunt, M. Munde, A. Kumar, M. A. Ismail, A. A. Farahat, R. K. Arafa, M. Say, A. Batista-Parra, D. Tevis, D. W. Boykin and W. D. Wilson, *Nucleic Acids. Res.*, 2011, **39**, 4265-4274.
5. E. P. Bishop, R. Rohs, S. C. J. Parker, S. M. West, P. Liu, R. S. Mann, B. Honig and T. D. Tullius, *ACS Chem. Biol.*, 2011, **6**, 1314-1320.
6. R. Tidwell and D. Boykin, in *Small molecule DNA and RNA binder: synthesis to nucleic acid complexes*, Wiley-VCH, New York, USA, 2003, pp. 416-460.
7. W. D. Wilson, F. A. Tanious, A. Mathis, D. Tevis, J. E. Hall and D. W. Boykin, *Biochimie*, 2008, **90**, 999-1014.
8. R. E. Jensen and P. T. Englund, *Annual review of microbiology*, 2012, **66**, 473-491.
9. C. Ríos Martínez, F. Miller, K. Ganeshamoorthy, F. Glacial, M. Kaiser, H. de Koning, A. Eze, L. Lagartera, T. Herraiz and C. Dardonville, *Antimicrob. Agents Chemother.*, 2015, **59**, 890-904.
10. C. H. Ríos Martínez, L. Lagartera, M. Kaiser and C. Dardonville, *Eur. J. Med. Chem.*, 2014, **81**, 481-491.
11. F. Rodríguez, I. Rozas, M. Kaiser, R. Brun, B. Nguyen, W. D. Wilson, R. N. García and C. Dardonville, *J. Med. Chem.*, 2008, **51**, 909-923.
12. C. Dardonville, M. P. Barrett, R. Brun, M. Kaiser, F. Tanious and W. D. Wilson, *J. Med. Chem.*, 2006, **49**, 3748-3752.
13. F. J. Acosta-Reyes, C. Dardonville, H. P. de Koning, M. Natto, J. A. Subirana and J. L. Campos, *Acta Cryst.*, 2014, **D70**, 1614-1621.
14. L. S. Glass, B. Nguyen, K. D. Goodwin, C. Dardonville, W. D. Wilson, E. C. Long and M. M. Georgiadis, *Biochemistry*, 2009, **48**, 5943-5952.
15. P. S. Nagle, F. Rodriguez, B. Nguyen, W. D. Wilson and I. Rozas, *J. Med. Chem.*, 2012, **55**, 4397-4406.
16. A. Kahvedžić, S.-M. Nathwani, D. M. Zisterer and I. Rozas, *J. Med. Chem.*, 2013, **56**, 451-459.
17. R. K. Arafa, M. A. Ismail, M. Munde, W. D. Wilson, T. Wenzler, R. Brun and D. W. Boykin, *Eur. J. Med. Chem.*, 2008, **43**, 2901-2908.
18. J. L. Gonzalez, C. E. Stephens, T. Wenzler, R. Brun, F. A. Tanious, W. D. Wilson, T. Barszcz, K. A. Werbovetz and D. W. Boykin, *Eur. J. Med. Chem.*, 2007, **42**, 552-557.
19. R. K. Arafa, R. Brun, T. Wenzler, F. A. Tanious, W. D. Wilson, C. E. Stephens and D. W. Boykin, *J. Med. Chem.*, 2005, **48**, 5480-5488.
20. B. Nguyen, F. A. Tanious and W. D. Wilson, *Methods*, 2007, **42**, 150-161.
21. W. D. Wilson, *Science*, 2002, **295**, 2103-2105.
22. R. A. Copeland, *Expert Opin. Drug Discov.*, 2010, **5**, 305-310.
23. R. A. Copeland, D. L. Pompliano and T. D. Meek, *Nat. Rev. Drug Discov.*, 2006, **5**, 730-739.
24. G. K. Walkup, Z. You, P. L. Ross, E. K. H. Allen, F. Daryaee, M. R. Hale, J. O'Donnell, D. E. Ehmann, V. J. A. Schuck, E. T. Buurman, A. L. Choy, L. Hajec, K. Murphy-Benenato, V. Marone, S. A. Patey, L. A. Grosser, M. Johnstone, S. G. Walker, P. J. Tonge and S. L. Fisher, *Nat. Chem. Biol.*, 2015, **11**, 416-423.
25. J. M. Bradshaw, J. M. McFarland, V. O. Paavilainen, A. Bisconte, D. Tam, V. T. Phan, S. Romanov, D. Finkle, J. Shu, V. Patel, T. Ton, X. Li, D. G. Loughhead, P. A. Nunn, D. E. Karr, M. E. Gerritsen, J. O. Funk, T. D. Owens, E. Verner, K. A. Brameld, R. J. Hill, D. M. Goldstein and J. Taunton, *Nat. Chem. Biol.*, 2015, **11**, 525-531.
26. M. Soler-López, L. Malinina and J. A. Subirana, *J. Biol. Chem.*, 2000, **275**, 23034-23044.
27. A. Sharma, K. R. Jenkins, A. Héroux and G. D. Bowman, *J. Biol. Chem.*, 2011, **286**, 42099-42104.
28. E. R. Johnson, S. Keinan, P. Mori-Sanchez, J. Contreras-Garcia, A. J. Cohen and W. Yang, *J. Am. Chem. Soc.*, 2010, **132**, 6498-6506.
29. The crystal structure of 5a bound to the DNA duplex (AAATTT)2 is currently being solved (Dr L. Campos and collaborators). This structure will be reported elsewhere.
30. F. Rodriguez, I. Rozas, J. E. Ortega, A. M. Erdozain, J. J. Meana and L. F. Callado, *J. Med. Chem.*, 2008, **51**, 3304-3312.
31. C. Dardonville, P. Goya, I. Rozas, A. Alsasua, M. I. Martin and M. J. Borrego, *Bioorg. Med. Chem.*, 2000, **8**, 1567-1577.
32. L. Nieto, A. Mascaraque, F. Miller, F. Glacial, C. Ríos Martínez, M. Kaiser, R. Brun and C. Dardonville, *J. Med. Chem.*, 2011, **54**, 485-494.
33. L. A. Mullice, R. H. Laye, L. P. Harding, N. J. Buurma and S. J. A. Pope, *New J. Chem.*, 2008, **32**, 2140-2149.
34. S. Mazur, F. A. Tanious, D. Ding, A. Kumar, D. W. Boykin, I. J. Simpson, S. Neidle and W. D. Wilson, *J Mol Biol*, 2000, **300**, 321-337.
35. Y. Liu, Y. Chai, A. Kumar, R. R. Tidwell, D. W. Boykin and W. D. Wilson, *J. Am. Chem. Soc.*, 2012, **134**, 5290-5299.
36. M. J. Frisch, G. W. Trucks, H. B. Schlegel, G. E. Scuseria, M. A. Robb, J. R. Cheeseman, G. Scalmani, V. Barone, B. Mennucci, G. A. Petersson, H. Nakatsuji, M. Caricato, X. Li, H. P. Hratchian, A. F. Izmaylov, J. Bloino, G. Zheng, J. L. Sonnenberg, M. Hada, M. Ehara, K. Toyota, R. Fukuda, J. Hasegawa, M. Ishida, T. Nakajima, Y. Honda, O. Kitao, H. Nakai, T. Vreven, J. Montgomery, J. A., J. E. Peralta, F. Ogliaro, M. Bearpark, J. J. Heyd, E. Brothers, K. N. Kudin, V. N. Staroverov, R. Kobayashi, J. Normand, K. Raghavachari, A. Rendell, J. C. Burant, S. S. Iyengar, J. Tomasi, M. Cossi, N. Rega, N. J. Millam, M. Klene, J. E. Knox, J. B. Cross, V. Bakken, C. Adamo, J. Jaramillo, R. Gomperts, R. E. Stratmann, O. Yazyev, A. J. Austin, R. Cammi, C. Pomelli, J. W. Ochterski, R. L. Martin, K. Morokuma, V. G. Zakrzewski, G. A. Voth, P. Salvador, J. J. Dannenberg, S. Dapprich, A. D. Daniels, Ö. Farkas, J. B. Foresman, J. V. Ortiz, J. Cioslowski and D. J. Fox, *Journal*, 2009.
37. A. D. Becke, *J. Chem. Phys.*, 1993, **98**, 5648-5652.
38. C. T. Lee, W. T. Yang and R. G. Parr, *Phys. Rev. B*, 1988, **37**, 785-789.
39. M. J. Frisch, J. A. Pople and J. S. Binkley, *J. Chem. Phys.*, 1984, **80**, 3265-3269.
40. O. Trott and A. J. Olson, *J. Comput. Chem.*, 2010, **31**, 455-461.
41. W. Humphrey, A. Dalke and K. Schulten, *J. Mol. Graphics*, 1996, **14**, 33-38.

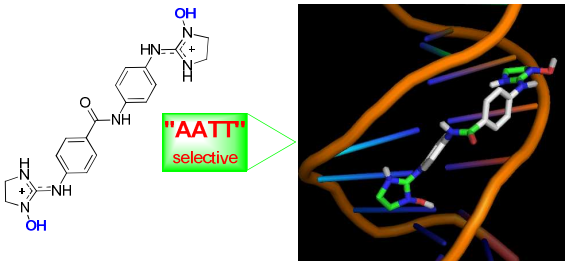

Selective binding of *N*-hydroxy bisimidazolines to dsDNA GCAATTGC derives from a tighter fit to this narrower minor groove.